


Article

An Improved Model–Free Current Predictive Control of Permanent Magnet Synchronous Motor Based on High–Gain Disturbance Observer

Yufeng Zhang *, Zihui Wu, Qi Yan, Nan Huang and Guanghui Du 

School of Electrical and Control Engineering, Xi'an University of Science and Technology, Xi'an 710054, China

* Correspondence: xkdzhangyufeng@xust.edu.cn

Abstract: Predictive current control (PCC) is an advanced control strategy for permanent magnet synchronous motors (PMSM). When the motor drive system is undisturbed, predictive current control exhibits a good dynamic response speed and steady–state performance, but the conventional PCC control performance of PMSM that depends on the motor body model is vulnerable to parameter perturbation. Aiming at this problem, an improved model–free predictive current control (IMFPCC) strategy based on a high–gain disturbance observer (HGDO) is proposed in this paper. The proposed strategy is introduced with the idea of model–free control, relying only on the system input and output to build an ultra–local current prediction model, which gets rid of the constraints of the motor body parameters. In the paper, the ultra–local structure is optimized by comparing and analyzing the equation of the state of the classical ultra–local structure and PMSM system. The system's current state variables are incorporated into the ultra–local system modeling, as a result, the current estimation errors existing in the classical ultra–local structure are eliminated. For the unmodeled and parametric perturbation part of the ultra–local system, a high–gain disturbance observer is designed to estimate it in real time. Finally, the proposed IMFPCC strategy is compared with the conventional model–based predictive current control (MPCC) and the conventional model–free predictive current control (CMFPCC) in simulation and experiment. The results show that the current steady–state error of the IMFPCC strategy in the case of parameter variation is only 50% of the MPCC method, which proves the effectiveness and correctness of the proposed strategy.

Keywords: permanent magnet synchronous motor; predictive current control; improved ultra–local model; high–gain disturbance observer



Citation: Zhang, Y.; Wu, Z.; Yan, Q.; Huang, N.; Du, G. An Improved Model–Free Current Predictive Control of Permanent Magnet Synchronous Motor Based on High–Gain Disturbance Observer. *Energies* **2023**, *16*, 141. <https://doi.org/10.3390/en16010141>

Academic Editors: José Gabriel Oliveira Pinto, Ping Liu, Yashan Hu, Jiangtao Yang and Jin Ye

Received: 4 November 2022

Revised: 24 November 2022

Accepted: 19 December 2022

Published: 23 December 2022



Copyright: © 2022 by the authors. Licensee MDPI, Basel, Switzerland. This article is an open access article distributed under the terms and conditions of the Creative Commons Attribution (CC BY) license (<https://creativecommons.org/licenses/by/4.0/>).

1. Introduction

PMSM is widely used in electric vehicles, aerospace, and intelligent manufacturing equipment because of its small size, high efficiency, and low noise [1]. Field Oriented Control (FOC) and Direct Torque Control (DTC) are the most commonly employed motor control strategies. However, they suffer from difficult parameter adjustment, large torque ripple, and poor robustness to achieve high–performance control of PMSM under complex operating conditions [2,3]. Therefore, the search for control strategies with better control performance and better robustness has become a hot issue of research in the field of PMSM drive.

Model–based predictive current control strategy (MPCC) has become a hot spot in the field of PMSM control in recent years due to its excellent dynamic response performance, simple and intuitive control idea, and significant advantages such as nonlinear multi–objective constraints [4–6]. The prediction system and the cost function are the core modules of model predictive control [7,8]. Although conventional model predictive control has a fast dynamic response, it has poor steady–state performance at low frequencies, and modulated model predictive control was proposed to optimize this problem [7]. The

adjustment of the valuation function allows predictive control to achieve synergistic optimization of multiple objectives. In [8], a Lyapunov energy function is proposed instead of the cost function to improve the global quality of motor control. Although MPCC has many advantages, it also has this fatal flaw. MPCC is extremely dependent on the motor body model. The control performance of conventional MPCC is easily affected by the change of motor parameters, which are bound to change during the actual operation of PMSM due to complex working conditions and other reasons. For this reason, scholars have conducted relevant studies on the effect of motor parameter drift on MPCC and its optimization methods [9–13]. A mathematical model between the stator current prediction error and parameter perturbations was presented in [10]. With the prediction error as the evaluation target, it is proved through theoretical analysis and experimental verification that the variation of inductor parameters has a large impact on motor performance, and the prediction error generated by the positive and negative inductance deviations in the $d-q$ axis is different. In [11], a self-tuning strategy for the mathematical model of the stator current was proposed, using the current prediction error to calculate the disturbances caused by the changes in the motor body parameters, and periodically correcting the current prediction model, which improves the robustness of the system to some extent. In [12], a high-order sliding mode observer was designed to observe the disturbances in the speed and current loops and feedback to the dual-loop controller, which improves the robustness of the system to some extent, but it still relies on all motor parameters to construct the predictive system. An inductance parameter compensation method was proposed in [13], which uses the prediction error to estimate inductance deviation information and thus perform inductance compensation. However, such online parameter identification methods usually have high requirements for controller performance.

To further suppress the influence of motor parameters, academics consider combining model-free control methods with PMSM drive systems. Incremental model-based predictive current control can estimate the motor current at the next moment without using any motor parameters, but the stator current needs to be collected twice in one control cycle, which has high system hardware requirements [14–16]. Ma improves on the incremental current prediction control by introducing a dual vector modulation method to reduce current ripple and improve current prediction accuracy by shortening the current ramp refresh period [17]. Although PCC based on an incremental model is not affected by motor parameters, it increases the hardware burden of the drive system to some extent.

Michel Fliess proposed a new model-free control idea based on the construction of an ultra-local model of the system input and output, which does not require concrete parameters of the control object and improves the parametric robustness of the control strategy [18]. The new model-free control idea was first introduced into the drive system of PMSM by Li's team, and a series of studies were conducted [19–21]. In [20], an ultra-local current model of a surface-mounted PMSM was constructed in conjunction with its mathematical model form, and model-free predictive current control of a surface-mounted PMSM was implemented. The effectiveness of the model-free control based on the ultra-local model is demonstrated in comparison with the traditional PI control strategy. Furthermore, model-free differential beat predictive speed control was proposed by Li, which verified the feasibility of applying the ultra-local model to the speed loop [21]. However, all of the above-proposed methods use the algebraic parameter identification method designed in [19] for the estimation of the unknown part of the ultra-local model, which requires collecting and storing the current and voltage of the motor for several cycles, which requires too much performance of the controller, and the accuracy of the disturbance estimation is not enough and fluctuates a lot. In [22], a dual-loop ultra-local prediction model for the speed and current loops of the PMSM control system is established, and the system is compensated for feedforward disturbances in real time with the help of an extended state observer (ESO) and a disturbance observation compensator (DOC), which improves the robustness and current tracking performance of the system. However, ESO tuning is more complex and not easy to achieve optimal control of the system. The inclusion of feedfor-

ward nonlinear disturbance compensation in model-free predictive control improves the dynamic performance of the system and reduces cross-direct-axis current harmonics [23]. A simplified model-free control strategy was proposed in the literature [24], which reduces the use of an extended Kalman filter (EKF) to estimate the unknown part of the ultra-local model by simplifying the voltage selection process, and the simulation results show that the EKF maintains strong robustness under various parameter variations. However, the design process of EKF is tedious and the Q and R matrices are extremely expensive to compute. Moreover, EKF is not applicable in some highly nonlinear systems [25]. To reduce the negative impact of permanent magnet demagnetization on the PMSM operation process, Zhao et al. proposed a robust model-free non-singular terminal sliding mode control (MFNTSMC) algorithm based on the ultra-local model [26]. The sliding mode observer does not depend on the system model and has a simple design with strong robustness, but due to its characteristics, it inevitably causes system jitter [27]. The high-gain observer is an effective method for asymptotic estimation of state quantities based on measurements [28]. The high-gain observer originates from the theory of output feedback suppression in nonlinear control. It is robust to modeling errors in the nonlinear part of the system and well suited for strongly coupled nonlinear permanent magnet synchronous motor systems [29,30]. High-gain designs are well suited to counteract external disturbances and modeling errors in permanent magnet synchronous motor drive systems, especially under time-varying, multivariable and parameter-unknown operating conditions [31].

To improve the parameter robustness and steady-state control performance of MPCC, an improved model-free predictive current control based on a high-gain disturbance observer (HGDO) is proposed in this paper. The proposed IMFPC strategy constructs the ultra-local current prediction model based only on the inputs and outputs of the drive system of the PMSM, which suppresses the effect of motor parameters change on the control performance. Unlike the classical ultra-local structure, the improved ultra-local model designed in this paper separates the current state variables from the unknown part and incorporates them into the ultra-local structure modeling. As a result, the errors between the current estimates and the actual values are eliminated, thus improving the accuracy of motor current prediction and reducing the system steady-state error. In addition, the HGDO that is independent of the exact model of the system is designed to estimate the unmodeled and parametrically perturbed part of the ultra-local system. Compared with the traditional algebraic parameter identification method, the HGDO does not need to collect the knowledge of the system input and output for the past several cycles, which greatly reduces the computational burden of the controller and improves the accuracy of the disturbance estimation. The proposed IMFPC strategy is proved to have strong robustness and good control performance by simulation and experiment.

The rest of the paper is organized as follows: the conventional model-free predictive current control is introduced in Section 2; the improved model-free predictive control current algorithm proposed in this paper, including the optimization of the classical ultra-local model and the derivation and modeling of HGDO, is presented in detail in Section 3. In Section 4, algorithm simulations and physical experiments are conducted to verify the dynamic and steady-state performance and parameter robustness of the proposed method. Finally, a summary and outlook of this work are presented in Section 5.

2. Conventional Model-Free Predictive Current Control

2.1. Mathematical Model of PMSM Considering Disturbance Factors

During the actual operation of the motor, the electrical parameter values of the motor body are easily affected by complex working conditions and extreme environments [32]. For the purpose of further improving the consistency between the mathematical model of PMSM and the actual operational model, the parameter perturbation term, the sys-

tem unmodeled term and the external disturbance term can be introduced into the ideal mathematical model of PMSM, then the mathematical model of PMSM can be rewritten as:

$$\begin{cases} u_d = (R_s + \Delta R)i_d + (L_d + \Delta L_d)\frac{di_d}{dt} - \omega_e(L_q + \Delta L_q)i_q + V_d + T_d \\ u_q = (R_s + \Delta R)i_q + (L_q + \Delta L_q)\frac{di_q}{dt} + \omega_e(L_d + \Delta L_d)i_d + \omega_e(\psi_f + \Delta\psi_f) + V_q + T_q \end{cases} \quad (1)$$

where u_d and u_q are the stator voltage components in the d and q axes, i_d and i_q are the stator current components in the d and q axes, R_s is the stator resistance; L_d and L_q are the inductance components in the d and q axes, ω_e is the electric angular velocity, is the permanent magnet chain, ΔR , ΔL_d , ΔL_q and $\Delta\psi_f$ are the motor parameter perturbation; V_d and V_q represent the unmodeled part of the d and q axes, T_d and T_q are the external disturbance terms in the d and q axes.

The total set disturbance of the motor in the d and q axes can be expressed as f_d and f_q :

$$\begin{cases} f_d = \Delta R i_d + \Delta L_d \frac{di_d}{dt} - \omega_e \Delta L_q i_q + V_d + T_d \\ f_q = \Delta R i_q + \Delta L_q \frac{di_q}{dt} + \omega_e \Delta L_d i_d + \omega_e \Delta \psi_f + V_q + T_q \end{cases} \quad (2)$$

Then Equation (1) can be simplified as:

$$\begin{cases} u_d = R_s i_d + L_d \frac{di_d}{dt} - \omega_e L_q i_q + f_d \\ u_q = R_s i_q + L_q \frac{di_q}{dt} + \omega_e L_d i_d + \omega_e \psi_f + f_q \end{cases} \quad (3)$$

2.2. Construction of Classical Ultra-Local Model for PMSM

The classical ultra-local model [19] of PMSM can be obtained from the mathematical model of PMSM considering the disturbance factors as:

$$\begin{bmatrix} di_d/dt \\ di_q/dt \end{bmatrix} = \begin{bmatrix} B_d & 0 \\ 0 & B_q \end{bmatrix} \begin{bmatrix} u_d \\ u_q \end{bmatrix} + \begin{bmatrix} F_d \\ F_q \end{bmatrix} \quad (4)$$

where B_d and B_q represent the scaling factors of the stator voltages in the d and q axes, which are usually constant and adjusted by the designer, F_d and F_q represent the unmodeled and total set disturbance parts in the d and q axes.

The estimates of F_d and F_q can be obtained by the algebraic parameter identification technique [19], as follows:

$$\begin{cases} \hat{F}_d = -\frac{3!}{T_F^3} \int_0^{T_F} ((T_F - 2\delta)i_d(\delta) + B_d\delta(T_F - \delta)u_d(\delta))d\delta \\ \hat{F}_q = -\frac{3!}{T_F^3} \int_0^{T_F} ((T_F - 2\delta)i_q(\delta) + B_q\delta(T_F - \delta)u_q(\delta))d\delta \end{cases} \quad (5)$$

where $T_F = n_F \cdot T_s$, n_F is the window sequence length. T_s is the control period. Here, the value of n_F is more critical, if the value of n_F is too large, the system computation will increase significantly, if the value of n_F is too small, the control performance of CMFPC may be greatly reduced, here $n_F = 5$.

2.3. Conventional Model-Free Predictive Current Control

When the control period T_s of the motor drive system is small enough, Equation (4) leads to the discretization of the ultra-local current prediction model as [19]:

$$\begin{cases} i_d^P(k+1) = (\hat{F}_d(k) + B_d u_d(k))T_s + i_d(k) \\ i_q^P(k+1) = (\hat{F}_q(k) + B_q u_q(k))T_s + i_q(k) \end{cases} \quad (6)$$

where $i_d(k)$ and $i_q(k)$ are the sampled currents of motor d and q axes at the moment k, $i_d^P(k+1)$ and $i_q^P(k+1)$ are the predicted motor currents at the moment (k + 1).

PCC takes the current as the optimization target, so the main purpose of the cost function is to make the predicted current at the next moment track the current reference value in the d and q axes, so it can be designed as:

$$g = \left| i_d^* - i_d^P(k+1) \right| + \left| i_q^* - i_q^P(k+1) \right| \quad (7)$$

where i_d^* and i_q^* represent the d and q axis current reference values.

3. Improved Model-Free Predictive Control of PMSM Based on High-Gain Disturbance Observer

3.1. Ultra-Local Model Optimization

It is obvious from the structure of the classical ultra-local model that the classical ultra-local model considers the motor current variables as an unknown part of the system for estimation. However, there is bound to be some error between the estimated current variable and the actual current variable. Since the manifestation of current state variables in the drive system of PMSM is known and the true value of current is measurable. Therefore, it can be separated from the unknown part and incorporated into the ultra-local modeling [33]; thus, the current state variable estimation error is eliminated and the motor current prediction accuracy is further improved. Then the classical ultra-local model can be rewritten as:

$$\begin{bmatrix} di_d/dt \\ di_q/dt \end{bmatrix} = \begin{bmatrix} A_d & 0 \\ 0 & A_q \end{bmatrix} \begin{bmatrix} i_d \\ i_q \end{bmatrix} + \begin{bmatrix} B_d & 0 \\ 0 & B_q \end{bmatrix} \begin{bmatrix} u_d \\ u_q \end{bmatrix} + \begin{bmatrix} E_d \\ E_q \end{bmatrix} \quad (8)$$

where A_d and A_q represent the current constant coefficients of d and q axes, B_d and B_q represent the voltage constant coefficients of d and q axes, E_d and E_q represent the unmodeled and total set disturbance parts of d and q axes.

3.2. Improved Model-Free Predictive Current Control

Equation (8) is discretized using the first-order forward Eulerian discretization, the improved model-free current prediction is obtained as follows:

$$\begin{bmatrix} i_d^P(k+1) \\ i_q^P(k+1) \end{bmatrix} = \begin{bmatrix} 1 + T_s A_d & 0 \\ 0 & 1 + T_s A_q \end{bmatrix} \begin{bmatrix} i_d(k) \\ i_q(k) \end{bmatrix} + \begin{bmatrix} B_d & 0 \\ 0 & B_q \end{bmatrix} \begin{bmatrix} u_d(k) \\ u_q(k) \end{bmatrix} + \begin{bmatrix} E_d(k) \\ E_q(k) \end{bmatrix} \quad (9)$$

where $i_d^P(k+1)$ and $i_q^P(k+1)$ denote the predicted currents in the d and q axes at the moment (k + 1), respectively.

The PCC algorithm in practice may lead to deviations in the predicted current at the next moment due to the delay in digital operations, so it is necessary to use a two-step prediction to make up for the digital delay. The implementation process is shown in Figure 1.

The current prediction after the delay compensation can be rewritten as:

$$\begin{bmatrix} i_d^P(k+2) \\ i_q^P(k+2) \end{bmatrix} = \begin{bmatrix} 1 + T_s A_d & 0 \\ 0 & 1 + T_s A_q \end{bmatrix} \begin{bmatrix} i_d(k+1) \\ i_q(k+1) \end{bmatrix} + \begin{bmatrix} B_d & 0 \\ 0 & B_q \end{bmatrix} \begin{bmatrix} u_d(k+1) \\ u_q(k+1) \end{bmatrix} + \begin{bmatrix} E_d(k+1) \\ E_q(k+1) \end{bmatrix} \quad (10)$$

The cost function after taking into account the delay compensation is rewritten as:

$$g = \left| i_d^* - i_d^P(k+2) \right| + \left| i_q^* - i_q^P(k+2) \right| \quad (11)$$

where $i_d^P(k+2)$ and $i_q^P(k+2)$ are the predicted values of the current at the moment (k + 2) of the d and q axes.

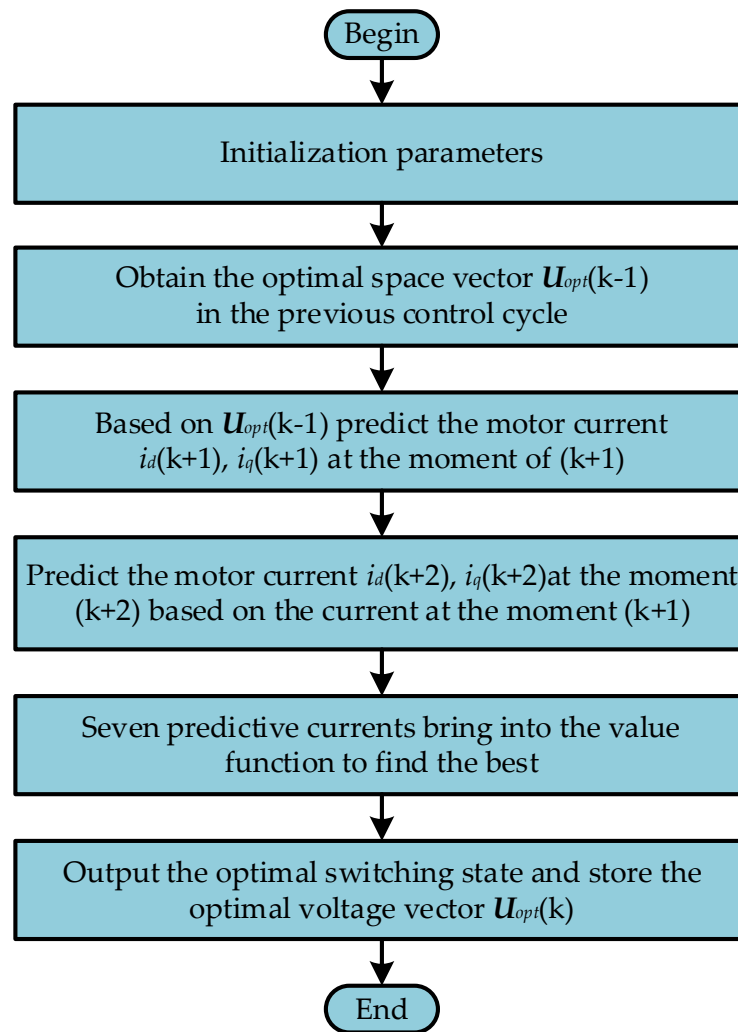


Figure 1. Flow chart of delayed compensation.

3.3. Design of High-Gain Disturbance Observer

The ability of the ultra-local model to approximate the actual operating motor drive system relies heavily on the accurate estimation of the unknown parts E_d and E_q . The traditional parameter identification method needs to collect the system input and output quantities for multiple control cycles, which is a large burden on the controller and the estimation accuracy is not high. Therefore, a high-gain disturbance observer is designed in this paper to estimate E_d and E_q periodically and accurately.

Based on Equation (8), E_d , E_q , i_d and i_q are defined as the system state variables, and the motor system state equation is rewritten as:

$$\begin{cases} \frac{dx}{dt} = Ax + Bu \\ y = Cx \end{cases} \quad (12)$$

$$\begin{aligned} A &= \begin{bmatrix} A_{dq} & I \\ 0 & 0 \end{bmatrix}, A_{dq} = \begin{bmatrix} A_d & 0 \\ 0 & A_q \end{bmatrix} \\ B &= \begin{bmatrix} B_{dq} & 0 \\ 0 & 0 \end{bmatrix}, B_{dq} = \begin{bmatrix} B_d & 0 \\ 0 & B_q \end{bmatrix} \\ C &= \begin{bmatrix} I & 0 \\ I & 0 \end{bmatrix} \end{aligned} \quad (13)$$

where $\mathbf{x} = [i_d \ i_q \ E_d \ E_q]^T$ are the state variables of the PMSM drive system, $\mathbf{u} = [u_d \ u_q \ 0 \ 0]^T$ are the input variables of the PMSM drive system, and $\mathbf{y} = [i_d \ i_q \ i_d \ i_q]^T$ are the output variables of the PMSM drive system.

The high-gain disturbance observer is constructed based on Equation (12):

$$\begin{cases} \frac{d\hat{\mathbf{x}}}{dt} = \mathbf{A}\hat{\mathbf{x}} + \mathbf{B}\mathbf{u} + \mathbf{H}(\mathbf{y} - \mathbf{C}\hat{\mathbf{x}}) \\ \hat{\mathbf{y}} = \mathbf{C}\hat{\mathbf{x}} \end{cases} \tag{14}$$

where the “^” sign represents the observed value, $\hat{\mathbf{x}} = [\hat{i}_d \ \hat{i}_q \ \hat{E}_d \ \hat{E}_q]^T, \hat{\mathbf{y}} = [\hat{i}_d \ \hat{i}_q \ \hat{i}_d \ \hat{i}_q]^T,$

$\mathbf{H} = \begin{bmatrix} h_1/\varepsilon & 0 & 0 & 0 \\ 0 & h_2/\varepsilon & 0 & 0 \\ 0 & 0 & h_3/\varepsilon^2 & 0 \\ 0 & 0 & 0 & h_4/\varepsilon^2 \end{bmatrix}.$ \mathbf{H} is the high-gain observation matrix, $h_1, h_2, h_3, h_4, \varepsilon$ are positive constants and $\varepsilon \ll 1.$

When the characteristic polynomial of $\tilde{\mathbf{A}} = \mathbf{A} - \mathbf{H}\mathbf{C}$ is a Hurwitz polynomial, then the observer is stable.

$$|s\mathbf{I} - \tilde{\mathbf{A}}| = m_4s^4 + m_3s^3 + m_2s^2 + m_1s + m_0 \tag{15}$$

$$\begin{cases} m_4 = 1 \\ m_3 = h_1/\varepsilon + h_2/\varepsilon - A_d - A_q \\ m_2 = (h_1/\varepsilon - A_d) + (h_2/\varepsilon - A_q) - h_3/\varepsilon^2 \\ m_1 = h_3/\varepsilon^2(h_2/\varepsilon - A_q) \\ m_0 = 0 \end{cases} \tag{16}$$

The Hurwitz determinant of the characteristic equation can be obtained as:

$$\Delta_4 = \begin{bmatrix} m_3 & m_1 & 0 & 0 \\ m_4 & m_2 & 0 & 0 \\ 0 & m_3 & m_1 & 0 \\ 0 & m_4 & m_2 & m_0 \end{bmatrix} \tag{17}$$

The observer system is globally stable when the main determinant of Δ_4 and its sequential main sub-formulae are all positive.

The high-gain disturbance observer constructed by Equation (14) is discretized:

$$\hat{\mathbf{x}}(k+1) = \mathbf{P}_M\hat{\mathbf{x}}(k) + \mathbf{B}'\mathbf{u}(k) + \mathbf{H}\mathbf{x}(k) \tag{18}$$

where $\hat{\mathbf{x}}(k+1) = [\hat{i}_d(k+1) \ \hat{i}_q(k+1) \ \hat{E}_d(k+1) \ \hat{E}_q(k+1)]^T,$
 $\hat{\mathbf{x}}(k) = [\hat{i}_d(k) \ \hat{i}_q(k) \ \hat{E}_d(k) \ \hat{E}_q(k)]^T, \mathbf{u}(k) = [u_d(k) \ u_q(k) \ 0 \ 0]^T,$
 $\mathbf{P}_M = \begin{bmatrix} (1 + T_s A_d - h_1/\varepsilon) & 0 & T_s & 0 \\ 0 & (1 + T_s A_q - h_2/\varepsilon) & 0 & T_s \\ -h_3/\varepsilon^2 & 0 & 1 & 0 \\ 0 & -h_4/\varepsilon^2 & 0 & 1 \end{bmatrix}, \mathbf{B}' = T_s \begin{bmatrix} \mathbf{B}_{dq} & \mathbf{0} \\ \mathbf{0} & \mathbf{0} \end{bmatrix}.$

4. Simulation and Experimental Verification

4.1. Simulation Analysis

The proposed IMFPC algorithm was compared and validated by MATLAB/Simulink. The simulated motor parameters are shown in Table 1.

Table 1. Nominal values of PMSM parameters.

Parameter	Symbol	Value
Rated voltage	U_N	380 V
Rated speed	n_N	1000 rpm
Rated torque	T_N	9.6 N·m
Stator resistance	R_s	3.95 Ω
Induction of d-axis	L_d	33.65 mH
Induction of q-axis	L_q	79.56 mH
Pole pairs	p	3
Magnetic flux	ψ_f	0.457 Wb

The control block diagram of the PMSM drive system is shown in Figure 2. A PI controller is used for the external speed loop and the IMFPCC controller is used for the internal current loop. The sampling frequency in the simulation is set to 10 kHz. The PI controller parameters K_p and K_i are set to 0.5 and 0.1, respectively, and the values of current and voltage coefficients in the IMFPCC controller are set to $A_d = -120$, $A_{dq} = 50$, $B_d = 30$, $B_q = 12$ after adjustment.

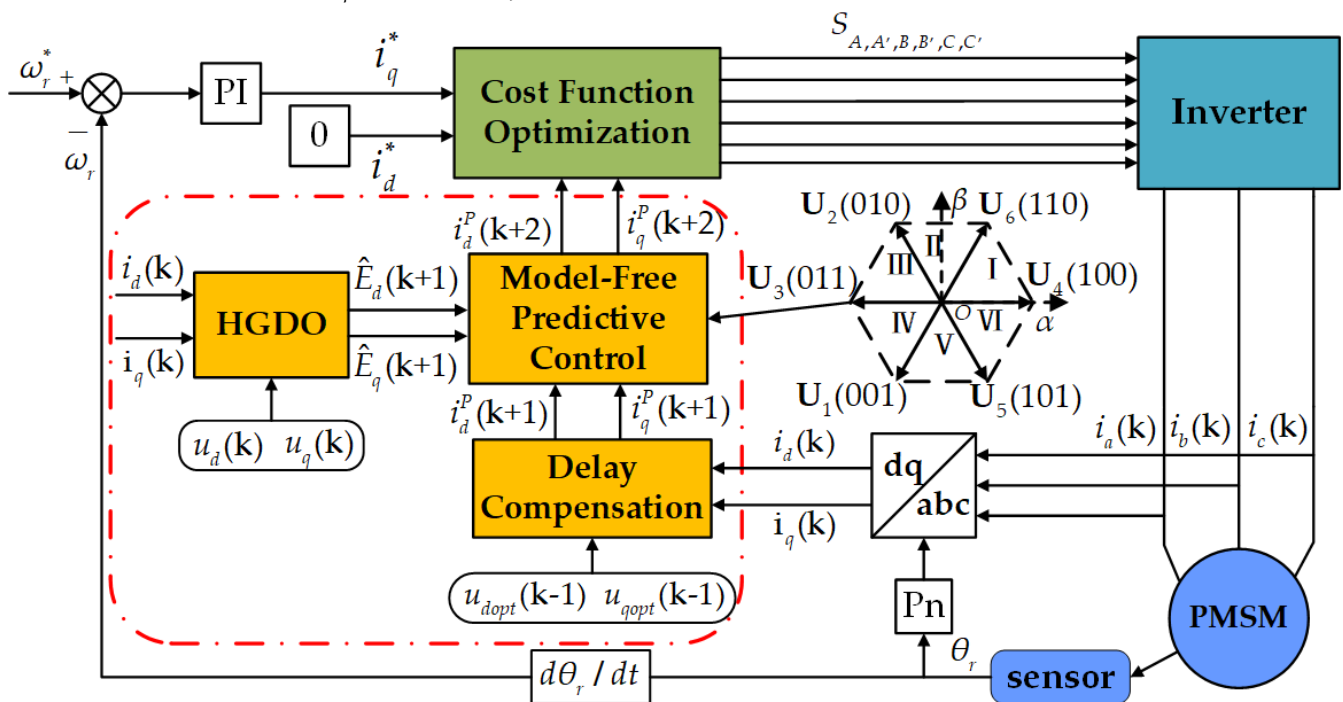


Figure 2. Block diagram of improved model-free predictive control system based on HGDO for PMSM.

In order to verify the correctness and superiority of the designed HGDO, simulations with continuous variations of motor parameters are performed in this section. MPCC and CMFPCC are compared with the proposed method in this paper for verification. The motor reference speed is set to 500 rpm with a load of 4 N·m. After the motor operation is stabilized, the motor parameters drop to $0.5 \cdot L_d$, $0.5 \cdot L_q$, and $0.5 \cdot R_s$, respectively, and recover to $1.0 \cdot L_d$, $1.0 \cdot L_q$, and $1.0 \cdot R_s$ after 0.4 s, and rise to $2.0 \cdot L_d$, $2.0 \cdot L_q$, and $2.0 \cdot R_s$ after 0.8 s. The simulation results are shown in Figure 3.

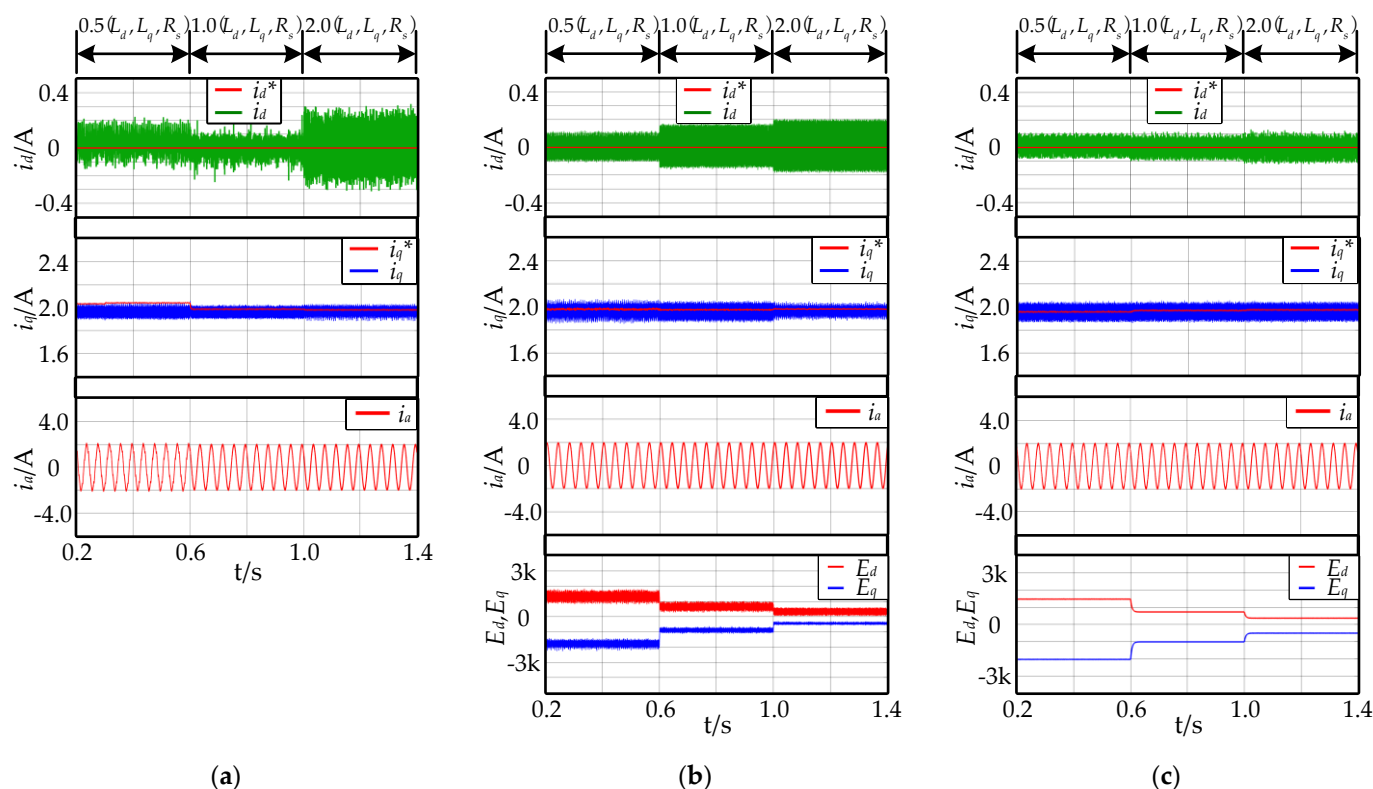


Figure 3. Simulation results of dq-axis current, phase current and dq-axis total disturbance under the change of motor parameters: (a) MPCC; (b) CMFPCC; (c) IMFPCC.

It is clear from Figure 3a that the conventional MPCC method is very sensitive to the changes in motor parameters, and the d–q axis currents all show a current shift from a given value and an increase in current ripple, indicating that parameter changes have a significant negative impact on the conventional MPCC strategy. On the other hand, the steady–state waveforms of CMFPCC and IMFPCC strategies under parameter variations are shown in Figure 3b,c, respectively. It is clearly seen that the motor maintains a relatively smooth static performance under the two model–free control strategies, the steady–state error of the three–phase current is very small, and the d–q currents follow the given values well. It can be seen from the changes in system disturbance observations that both strategies can detect the system disturbance caused by the internal parameter perturbation of the motor in time. However, the disturbance estimation accuracy of HGDO designed in this paper is significantly higher than that of the conventional algebraic parameter identification method. It improves the steady–state performance on the basis of ensuring the robustness of the motor drive system. The effectiveness and superiority of the designed high–gain disturbance observer are demonstrated.

The Fourier analysis of the A–phase currents for the three control strategies is shown in Figure 4. It is observed that the phase current THD of IMFPCC is 2.85% when the controller parameters are $0.5 \cdot (L_d, L_q, R_s)$ and 4.19% when the controller parameters are $2.0 \cdot (L_d, L_q, R_s)$. As can be seen, the proposed strategy can effectively suppress the negative effects of motor parameter changes when the motor parameters are not matched. When the motor parameters are matched, the THD of the three methods MPCC, CMFPCC and IMFPCC are 4.52%, 4.62% and 4.02%, respectively. It is clear that the steady–state performance of the CMFPCC method is worse than the other two methods, which is consistent with the previous analysis that the classical ultra–local structure ignores the current state variables and thus negatively affects the motor control performance.

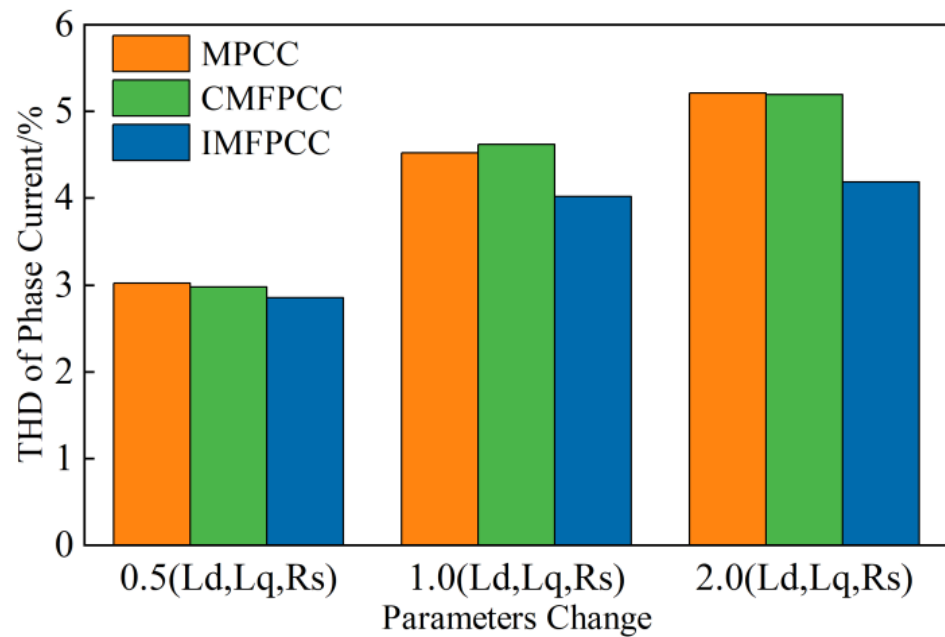


Figure 4. Comparison chart of phase current FFT analysis under parameters change.

4.2. Experimental Verification

In order to further validate the practicability and effectiveness of the algorithm proposed in this paper, physical experiments are carried out in this section. The Yanxu SP2000–based PMSM control drive platform is built, as shown in Figure 5, and the motor parameters are shown in Table 1. The sampling frequency in the experiment is also set to 10 kHz. Experimental data are collected and stored by the host computer and imported into MATLAB for analysis.

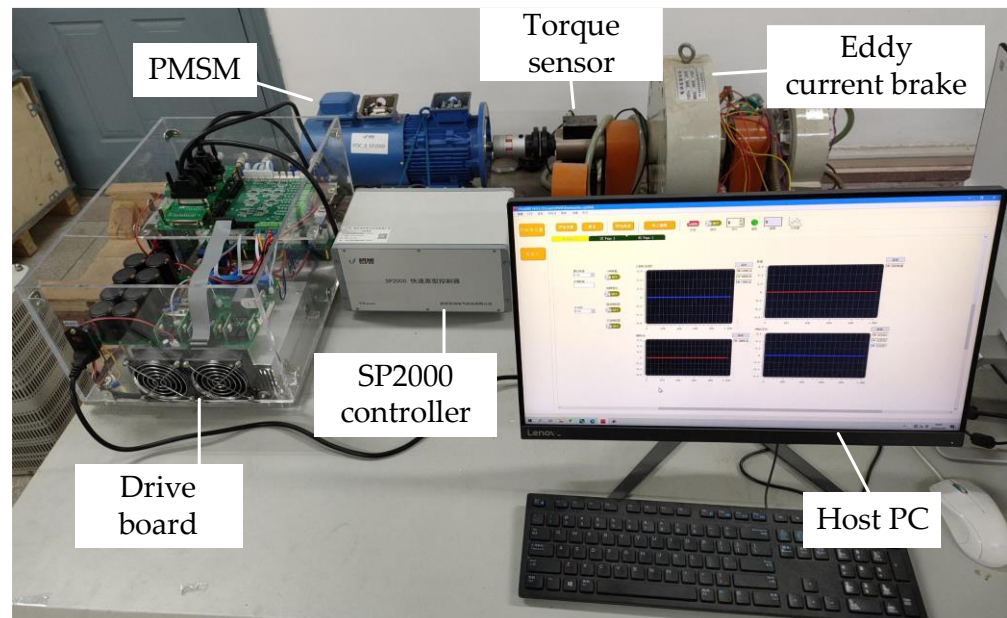


Figure 5. Experimental platform.

To verify the steady–state performance of the IMFPCC strategy with matched motor parameters, a comparison experiment is conducted with the conventional MPCC and CMFPCC methods. The motor operating conditions are set to 1000 rpm with a load of 9.6 N·m. The experimental waveforms are shown in Figure 6.

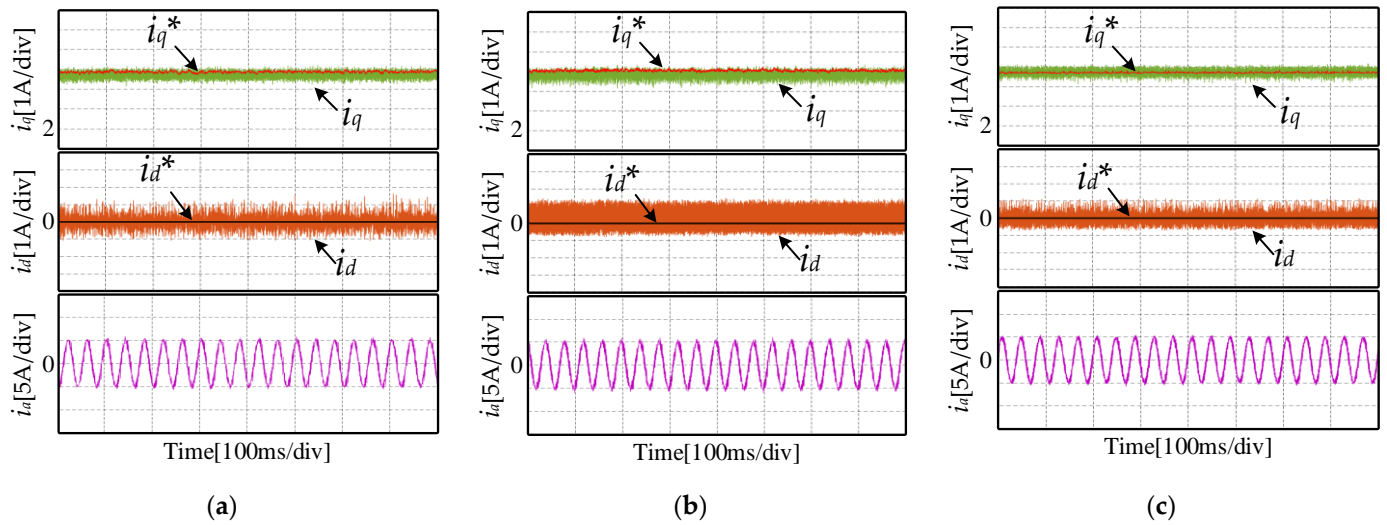


Figure 6. Experimental results of dq-axis current and phase current under matched motor parameters: (a) MPCC; (b) CMFPCC; (c) IMFPCC.

The comparison of the three subplots in Figure 6a–c shows that the steady-state current ripple of the MPCC strategy and the proposed IMFPCC strategy are similar when the motor parameters are matched. The steady-state current ripple of the CMFPCC strategy is the largest. The phase current FFT analysis in Figure 7 shows the current THD of 17.89% and 16.52% for the two, respectively. It proves that the three-phase current ripple of IMFPCC is slightly smaller than that of conventional MPCC. The steady-state current ripple of the CMFPCC strategy based on the classical ultra-local structure is significantly higher than that of the IMFPCC strategy based on the optimized ultra-local structure, and its phase current THD is as high as 19.13%.

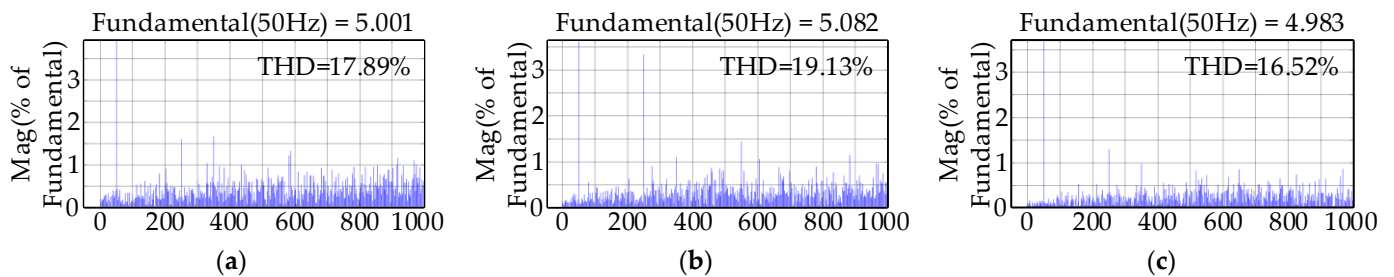


Figure 7. Phase current Fourier analysis of three control strategies under matched motor parameters: (a) MPCC; (b) CMFPCC; (c) IMFPCC.

Figure 8 shows the steady-state experimental results of the three control strategies when the motor parameters are varied from $0.5*(L_d, L_q, R_s)$ to $2.0*(L_d, L_q, R_s)$ in the controller. The motor operating condition is set to 600 rpm with a load of 5 N·m.

As can be seen in Figure 8a, the dq-axis current of the conventional MPCC deviates from the given value and the steady-state error increases when the motor parameters are continuously varied. When the motor parameters are larger than the controller parameters, the dq-axis steady-state current does not follow the reference value correctly, resulting in a considerable increase in the low-frequency harmonics of the current. When the motor parameters are smaller than the controller parameters, the current steady-state error of MPCC increases significantly with d-axis current ripple up to 1.8 A. This is because the model-based predictive current is inaccurate due to the mismatch of the motor parameters, which prevents the controller from selecting the optimal switching state for the next cycle. In contrast, the steady-state d-axis current ripple of the proposed IMFPCC is 0.9 A, which is only 50% of the conventional MPCC method. Figure 9 shows the THD values of the three

methods for the variation of motor parameters, and it can be clearly seen that IMFPPC has the smallest total harmonic distortion rate of the three—phase currents, which proves the superiority of the proposed strategy. In summary, the results show that both CMFPCC and IMFPPC can ensure stable motor control performance when the motor parameters are not matched, but the steady—state error of the proposed strategy is significantly better than that of CMFPCC. It proves the effectiveness of the proposed improved ultra—local model in this paper.

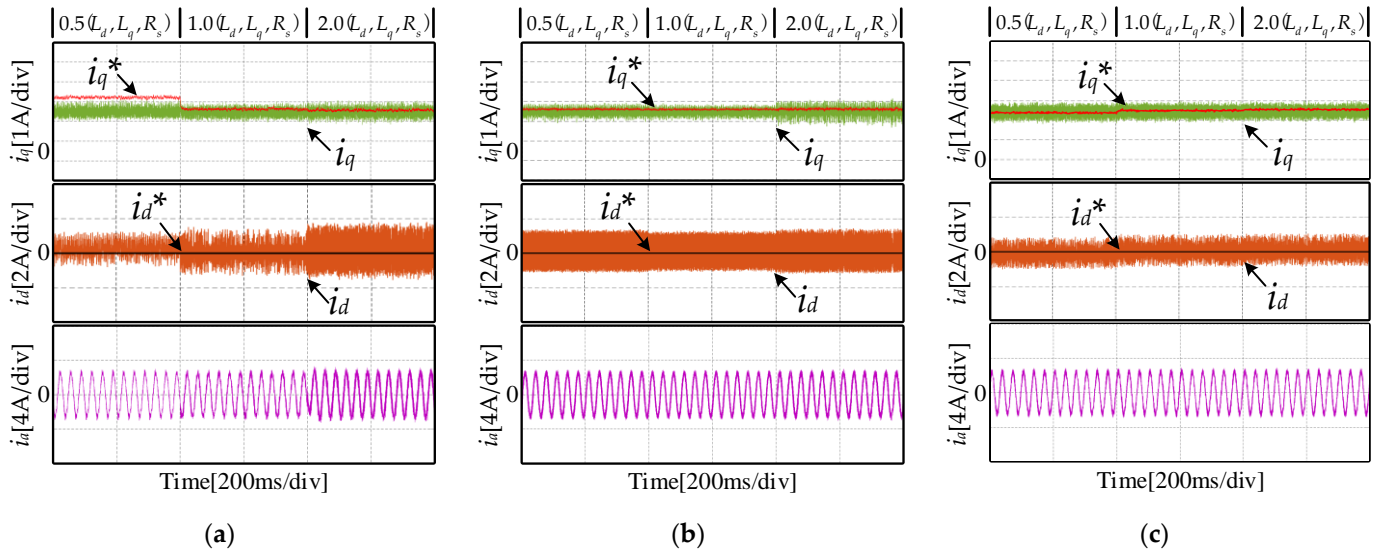


Figure 8. Experimental results of dq—axis current and phase current under mismatched motor parameters: (a) MPCC; (b) CMFPCC; (c) IMFPPC.

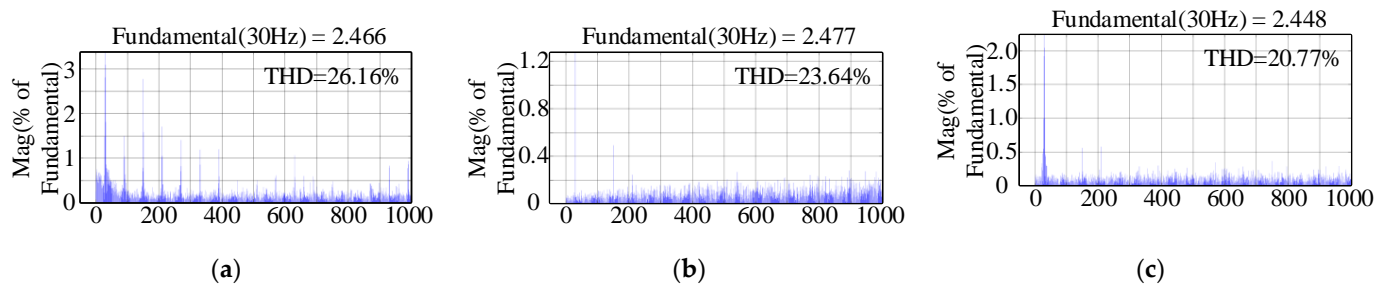


Figure 9. Phase current Fourier analysis of three control strategies under mismatched motor parameters: (a) MPCC; (b) CMFPCC; (c) IMFPPC.

In order to verify the dynamic performance of the proposed strategy and the stability of HGDO under the extreme operating conditions of the motor. Experiments of load addition and reduction, brief overloads and brief overspeeds were performed. In the experiment, the motor is initially operated at 600 rpm with a load of 5 N·m, then the load increases to 11.5 N·m ($1.2 \cdot T_N$), and after a brief overload, the motor load is reduced to 5 N·m again, and the speed command is increased from 600 rpm to 1200 rpm ($1.2 \cdot n_N$) after a period of time. The dynamic experimental waveforms of the three control strategies are given in Figure 10.

As shown in Figure 10, the dynamic response speed of the three methods is similar for the same load variation. It can be seen from the dq—axis current comparison that the MPCC and CMFPCC methods produce certain current fluctuations during acceleration. In contrast, the dynamic process of the proposed IMFPPC is smooth, allowing the motor to maintain a stable operating condition. The observation plots of disturbances in Figure 10b,c show that both CMFPCC and IMFPPC can estimate the external load disturbances during loading. However, it is obvious that the HGDO designed in this paper has higher accuracy

in disturbance estimation. In summary, the proposed IMFPC strategy exhibits superior dynamic performance under loading and ramp-up conditions.

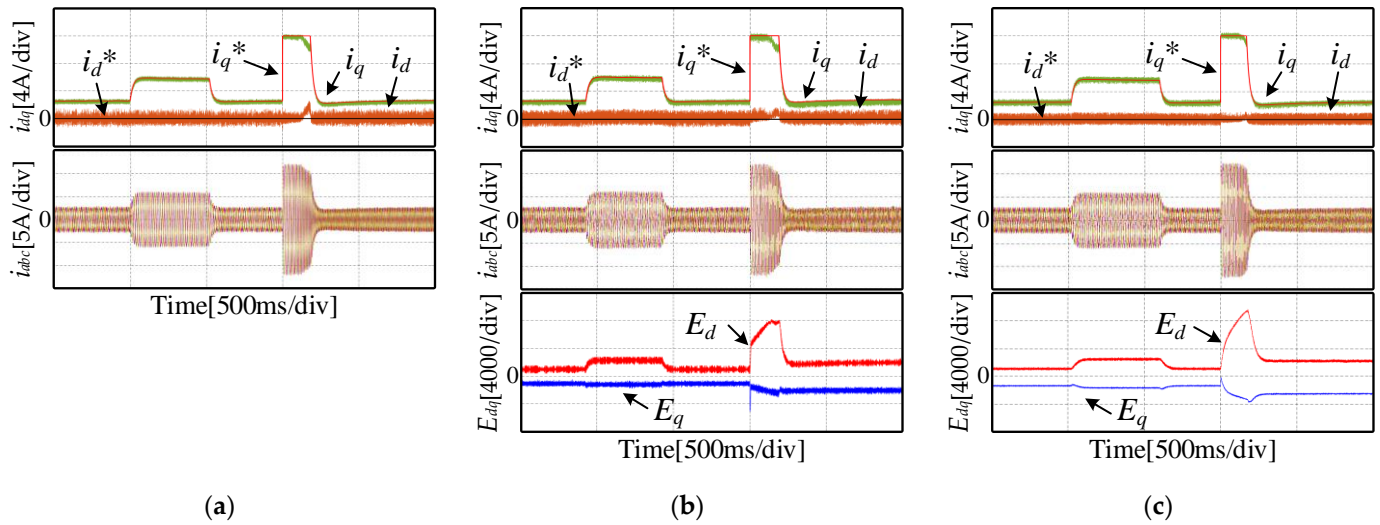


Figure 10. Experimental results of dq axis currents, phase currents and dq-axis total disturbance under dynamic working conditions: (a) MPCC; (b) CMFPC; (c) IMFPC.

Figure 11 shows the experimental waveform of motor forward and reverse rotation under the motor parameters change. The specific working condition is that the motor speed changes from 1000 rpm to -1000 rpm with a load of 5 N·m. The motor parameters change from $0.5 \cdot (L_d, L_q, R_s)$ to $2.0 \cdot (L_d, L_q, R_s)$. It can be seen that the current of MPCC and CMFPC has a large error during forward and reverse rotation when the parameters are not matched. In contrast, the dynamic waveform of IMFPC is smooth and has less error.

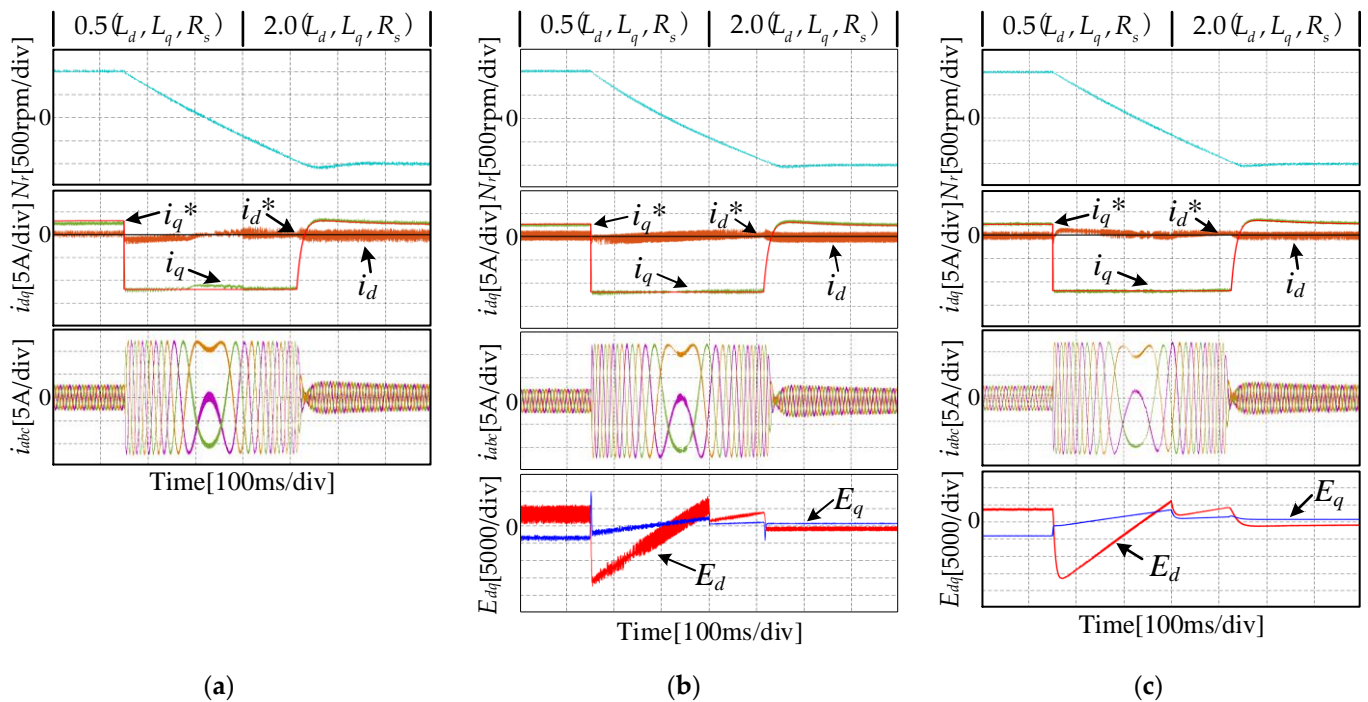


Figure 11. Experimental results of forward and reverse rotation under the change of motor parameters: (a) MPCC; (b) CMFPC; (c) IMFPC.

In order to compare the computation of the three algorithms, the algorithm controller processing time is further analyzed, and the results are shown in Table 2. As can be

seen from Table 2, the running time of the proposed algorithm and the traditional MPCC algorithm is basically the same. The CMFPCC algorithm time is significantly higher than the other two methods, which is mainly due to the increase in the controller burden by the disturbance estimation strategy based on the parameter identification method.

Table 2. Processing time of the controller for the three algorithms.

Control Algorithm	MPCC	CMFPCC	IMFPCC
Processing time of the controller/ μs	44	55	42

5. Conclusions

To address the problems of motor parameters sensitivity and low system robustness in predictive current control of PMSM, an improved model-free predictive current control that suppresses the motor body parameters and external disturbances are proposed in this paper. The proposed strategy does not rely on motor parameters to construct the current prediction model, which suppresses the effects of motor parameter variations and uncertainty disturbances on motor control performance. Compared with the classical ultra-local structure, the proposed strategy separates the motor current state variables from the unknown part, which improves the accuracy of the current prediction system and enhances the steady-state performance of the motor. For the unknown part of the ultra-local system, a high-gain disturbance observer is designed for estimation. Compared with the traditional parameter identification estimation method, the proposed disturbance observer does not increase the system hardware cost and has higher disturbance estimation accuracy, which is beneficial for practical engineering applications. Simulation and experimental results show: (1) The proposed IMFPCC strategy has a similar control effect with the conventional MPCC in the case of unregulated motor parameters, but the steady-state performance of IMFPCC is slightly better than the conventional MPCC method. The CMFPCC method has a larger current steady-state error compared to the other two methods. (2) The steady-state error and dynamic performance of the IMFPCC are better than those of the conventional MPCC and CMFPCC under the applied external load disturbance and inductor parameter variation, which verifies the effectiveness of the proposed IMFPCC method. The HGDO proposed in the paper reduces the controller computational burden and optimizes the disturbance estimation accuracy. However, it increases the control parameters and system tuning workload, so a series of studies will be conducted in the future around reducing the control parameters of HGDO.

Author Contributions: Conceptualization, Y.Z. and Z.W.; Data curation, Y.Z. and Z.W.; Formal analysis, Z.W.; Funding acquisition, G.D.; Investigation, Y.Z. and Z.W.; Methodology, Y.Z. and Z.W.; Project administration, Y.Z.; Resources, Y.Z.; Software, Z.W.; Supervision, Y.Z.; Validation, Y.Z., Q.Y., N.H. and G.D.; Visualization, Z.W.; Writing—original draft, Z.W.; Writing—review and editing, Y.Z., Z.W. and G.D. All authors have read and agreed to the published version of the manuscript.

Funding: This research was funded by National Nature Science Foundation of China, grant number 52177056.

Data Availability Statement: Not applicable.

Conflicts of Interest: The authors declare no conflict of interest.

References

1. Ilioudis, V.C. Sensorless Control of Permanent Magnet Synchronous Machine with Magnetic Saliency Tracking Based on Voltage Signal Injection. *Machines* **2020**, *8*, 14. [[CrossRef](#)]
2. Casadei, D.; Profumo, F.; Serra, G.; Tani, A. FOC and DTC: Two Viable Schemes for Induction Motors Torque Control. *IEEE Trans. Power Electron.* **2002**, *17*, 779–787. [[CrossRef](#)]
3. Xiong, C.; Xu, H.; Guan, T.; Zhou, P. A Constant Switching Frequency Multiple-Vector-Based Model Predictive Current Control of Five-Phase PMSM With Non-sinusoidal Back EMF. *IEEE Trans. Ind. Electron.* **2020**, *67*, 1695–1707. [[CrossRef](#)]

4. Agoro, S.; Husain, I. Robust Deadbeat Finite–Set Predictive Current Control with Torque Oscillation and Noise Reduction for PMSM Drives. *IEEE Trans. Ind. Appl.* **2022**, *58*, 365–374. [[CrossRef](#)]
5. Zhao, L.; Chen, Z.; Wang, H.; Li, L.; Mao, X.; Li, Z.; Zhang, J.; Wu, D. An Improved Deadbeat Current Controller of PMSM Based on Bilinear Discretization. *Machines* **2022**, *10*, 79. [[CrossRef](#)]
6. Gong, C.; Hu, Y.; Ma, M.; Yan, L.; Liu, J.; Wen, H. Accurate FCS Model Predictive Current Control Technique for Surface–Mounted PMSMs at Low Control Frequency. *IEEE Trans. Power Electron.* **2020**, *35*, 5567–5572. [[CrossRef](#)]
7. Körpe, U.U.; Gökdağ, M.; Koç, M.; Gülbudak, O. Modulated Model Predictive Torque Control for Interior Permanent Magnet Synchronous Machines. *El–Cezeri* **2022**, *9*, 777–787. [[CrossRef](#)]
8. Gulbudak, O.; Gokdag, M.; Komurcugil, H. Model Predictive Control Strategy for Induction Motor Drive Using Lyapunov Stability Objective. *IEEE Trans. Ind. Electron.* **2022**, *69*, 12119–12128. [[CrossRef](#)]
9. Turker, T.; Buyukkeles, U.; Bakan, A.F. A Robust Predictive Current Controller for PMSM Drives. *IEEE Trans. Ind. Electron.* **2016**, *63*, 3906–3914. [[CrossRef](#)]
10. Li, J.; Huang, X.; Niu, F.; You, C.; Wu, L.; Fang, Y. Prediction Error Analysis of Finite–Control–Set Model Predictive Current Control for IPMSMs. *Energies* **2018**, *11*, 2051. [[CrossRef](#)]
11. Wang, F.; Zuo, K.; Tao, P.; Rodriguez, J. High Performance Model Predictive Control for PMSM by Using Stator Current Mathematical Model Self–Regulation Technique. *IEEE Trans. Power Electron.* **2020**, *35*, 13652–13662. [[CrossRef](#)]
12. Zhang, X.; Hou, B.; Mei, Y. Deadbeat Predictive Current Control of Permanent–Magnet Synchronous Motors with Stator Current and Disturbance Observer. *IEEE Trans. Power Electron.* **2017**, *32*, 3818–3834. [[CrossRef](#)]
13. Liu, S.; Liu, C. Virtual–Vector–Based Robust Predictive Current Control for Dual Three–Phase PMSM. *IEEE Trans. Ind. Electron.* **2021**, *68*, 2048–2058. [[CrossRef](#)]
14. Lin, C.-K.; Liu, T.-H.; Yu, J.; Fu, L.-C.; Hsiao, C.-F. Model–Free Predictive Current Control for Interior Permanent–Magnet Synchronous Motor Drives Based on Current Difference Detection Technique. *IEEE Trans. Ind. Electron.* **2014**, *61*, 667–681. [[CrossRef](#)]
15. Da Ru, D.; Polato, M.; Bolognani, S. Model–Free Predictive Current Control for a SynRM Drive Based on an Effective Update of Measured Current Responses. In Proceedings of the 2017 IEEE International Symposium on Predictive Control of Electrical Drives and Power Electronics (PRECEDE), Pilsen, Czech Republic, 4–6 September 2017; pp. 119–124.
16. Ma, C.; Li, H.; Yao, X.; Zhang, Z.; De Belie, F. An Improved Model–Free Predictive Current Control with Advanced Current Gradient Updating Mechanism. *IEEE Trans. Ind. Electron.* **2021**, *68*, 11968–11979. [[CrossRef](#)]
17. Ma, C.; Rodriguez, J.; Garcia, C.; De Belie, F. Integration of Reference Current Slope Based Model–Free Predictive Control in Modulated PMSM Drives. *IEEE J. Emerg. Sel. Topics Power Electron.* **2022**. [[CrossRef](#)]
18. Fliess, M.; Join, C. Model–Free Control. *Int. J. Control* **2013**, *86*, 2228–2252. [[CrossRef](#)]
19. Zhou, Y.; Li, H.; Yao, H. Model–Free Control of Surface Mounted PMSM Drive System. In Proceedings of the 2016 IEEE International Conference on Industrial Technology (ICIT), Taipei, Taiwan, 14–17 March 2016; pp. 175–180.
20. Zhou, Y.; Li, H.; Zhang, H. Model–Free Deadbeat Predictive Current Control of a Surface–Mounted Permanent Magnet Synchronous Motor Drive System. *J. Power Electron.* **2018**, *18*, 103–115.
21. Zhou, Y.; Li, H.; Zhang, H.; Mao, J.; Huang, J. Model Free Deadbeat Predictive Speed Control of Surface–Mounted Permanent Magnet Synchronous Motor Drive System. *J. Electr. Eng. Technol.* **2019**, *14*, 265–274. [[CrossRef](#)]
22. Xu, L.; Chen, G.; Li, Q. Cascaded Speed and Current Model of PMSM with Ultra–local Model–free Predictive Control. *IET Electric Power Appl.* **2021**, *15*, 1424–1437. [[CrossRef](#)]
23. Xu, L.; Chen, G.; Li, Q. Ultra–Local Model–Free Predictive Current Control Based on Nonlinear Disturbance Compensation for Permanent Magnet Synchronous Motor. *IEEE Access* **2020**, *8*, 127690–127699. [[CrossRef](#)]
24. Zerdali, E.; Wheeler, P. Model–Free Simplified Predictive Current Control of PMSM Drive with Ultra–Local Model–Based EKF. In Proceedings of the 2021 3rd Global Power, Energy and Communication Conference (GPECOM), Antalya, Turkey, 5–8 October 2021; pp. 62–66.
25. Cao, R.; Jiang, N.; Lu, M. Sensorless Control of Linear Flux–Switching Permanent Magnet Motor Based on Extended Kalman Filter. *IEEE Trans. Ind. Electron.* **2020**, *67*, 5971–5979. [[CrossRef](#)]
26. Zhao, K.; Yin, T.; Zhang, C.; He, J.; Li, X.; Chen, Y.; Zhou, R.; Leng, A. Robust Model–Free Nonsingular Terminal Sliding Mode Control for PMSM Demagnetization Fault. *IEEE Access* **2019**, *7*, 15737–15748. [[CrossRef](#)]
27. Wang, Y.; Lan, Z.; Zhu, G. Adaptive Sliding Mode Observer Based on Phase Locked Loop in Sensorless Control of Permanent Magnet Linear Synchronous Motor. In Proceedings of the 2021 13th International Symposium on Linear Drives for Industry Applications (LDIA), Wuhan, China, 1–3 July 2021; pp. 1–6.
28. Liu, H.; Sun, J.; Nie, J.; Chen, G.; Zou, L. Adaptive Non–Singular Terminal Sliding Mode Control with High–Gain Observers for Robotic Manipulators. In Proceedings of the 2019 Chinese Control and Decision Conference (CCDC), Nanchang, China, 3–5 June 2019; pp. 3547–3552.
29. Zhou, Y.; Soh, Y.C.; Shen, J.X. High–Gain Observer with Higher Order Sliding Mode for State and Unknown Disturbance Estimations: High–Gain Observer with High Order Sliding Mode. *Int. J. Robust. Nonlinear Control* **2014**, *24*, 2136–2151. [[CrossRef](#)]
30. Wang, L.J.; Zhao, J.W.; Dong, F.; He, Z.Y.; Song, J.C.; Li, M. High–bandwidth and Strong Robust Predictive Current Control Strategy Research for Permanent Magnet Synchronous Linear Motor Based on Adaptive Internal Model Observer. *Proc. CSEE* **2019**, *39*, 3098–3107. (In Chinese)

31. Won, D.; Kim, W.; Shin, D.; Chung, C.C. High-Gain Disturbance Observer-Based Backstepping Control with Output Tracking Error Constraint for Electro-Hydraulic Systems. *IEEE Trans. Contr. Syst. Technol.* **2015**, *23*, 787–795. [[CrossRef](#)]
32. Zhang, X.; Zhang, L.; Zhang, Y. Model Predictive Current Control for PMSM Drives with Parameter Robustness Improvement. *IEEE Trans. Power Electron.* **2019**, *34*, 1645–1657. [[CrossRef](#)]
33. Safaei, A.; Mahyuddin, M.N. Adaptive Model-Free Control Based on an Ultra-Local Model with Model-Free Parameter Estimations for a Generic SISO System. *IEEE Access* **2018**, *6*, 4266–4275. [[CrossRef](#)]

Disclaimer/Publisher’s Note: The statements, opinions and data contained in all publications are solely those of the individual author(s) and contributor(s) and not of MDPI and/or the editor(s). MDPI and/or the editor(s) disclaim responsibility for any injury to people or property resulting from any ideas, methods, instructions or products referred to in the content.